Chapter 14

Can linear collocation ever beat quadratic?

Rebecca Martin, David J. Chappell, Nadia Chuzhanova and Jonathan J. Crofts

Department of Mathematics and Physics,
Nottingham Trent University
Nottingham
UK

Abstract. *Computational approaches are becoming increasingly important in neuroscience, where complex, nonlinear systems modelling neural activity across multiple spatial and temporal scales are the norm. This paper considers collocation techniques for solving neural field models, which typically take the form of a partial integro-differential equation. In particular, we investigate and compare the convergence properties of linear and quadratic collocation on both regular grids and more general meshes not fixed to the regular Cartesian grid points. For regular grids we perform a comparative analysis against more standard techniques, in which the convolution integral is computed either by using Fourier based methods or via the trapezoidal rule. Perhaps surprisingly, we find that on regular, periodic meshes, linear collocation displays better convergence properties than quadratic collocation, and is in fact comparable with the spectral convergence displayed by both the Fourier based and trapezoidal techniques. However, for more general meshes we obtain superior convergence of the convolution integral using higher order methods, as expected.*

14.1   Introduction

Neural field theory employs a continuum approach to model the activity of large populations of neurons in the cortex [1]. Such models are of great interest, not only from a mathematical point of view, but also from an experimental neuroscience point of view, since they are capable of replicating experimentally observed patterns of brain activity [2, 3]. Typically, such models take the form of a non-linear partial integro-differential equation such as

$$\frac{\partial}{\partial t}u(\mathbf{x}, t) = -u(\mathbf{x}, t) + \int_{\Omega} w(\mathbf{x} - \mathbf{x}')S(u(\mathbf{x}'))d\mathbf{x}'. \tag{14.1}$$

Here $u(\mathbf{x}, t)$ describes the average activity of the neuronal population at position $\mathbf{x} \in \Omega$ at time t, while the nonlinear function S represents the mean firing rate, and typically takes the form of a sigmoid function. The connectivity kernel, w, describes how neurons positioned at $\mathbf{x}$ and $\mathbf{x}'$ interact [4]. Note that for special choices of the integral kernel, the neural field model (NFM) in (14.1) can be reduced to a partial differential equation (PDE), and the theory and tools of

PDEs can be deployed to investigate its solutions [5]. However, when considering more general, physiologically realistic kernels, the determination of solutions and their subsequent analysis requires numerical techniques.

In this work, we consider a two-dimensional NFM of the form (14.1) adapted so as to include a recovery variable, which acts to repolarise neuronal activity via negative feedback, as in [6]. Thus, we consider the following coupled system of equations

$$\frac{\partial u(x,y,t)}{\partial t} = A \int_{-L}^{L} \int_{-L}^{L} w(x-x', y-y') S(u(x',y',t) - h) \mathrm{d}x' \mathrm{d}y'$$
$$\qquad\qquad - u(x,y,t) - a(x,y,t), \qquad\qquad\qquad (14.2)$$
$$\tau \frac{\partial a(x,y,t)}{\partial t} = B u(x,y,t) - a(x,y,t).$$

Here, $u(x,y,t)$ denotes population activity and $a(x,y,t)$ the recovery variable, at position (x,y) and time t. The parameters A, B, h and τ are related to the sensitivities and time-scale of the problem [6], and we set $\Omega = [-L, L]^2$ and impose periodic boundary conditions in both x and y for all of our experiments.

The role of S is to convert population activity into firing frequency, and it does this at a rate governed by the steepness parameter β [1]. Explicitly, S takes the form of a sigmoid with "steepness" parameter β as follows

$$S(u) = \frac{1}{1 + e^{-\beta u}}.$$

The integral kernel $w(x-x', y-y')$ describes interactions between neighbouring neurons, as described earlier, and in our work is set to be a Mexican-hat type function

$$w(x,y) = e^{-(x^2+y^2)} - 0.17 e^{-0.2(x^2+y^2)}.$$

The main source of error in the numerical approximation of Equation (14.2) is the convolution integral and so here we propose collocation techniques as a method for evaluating this integral. The main advantage of such a choice is that it can be directly generalised to the more general, typically asymmetric domains that result from modern neuroimaging studies. For completeness, we compare our results against standard techniques that typically use either Fourier based methods or the trapezoidal rule to compute the convolution integral in (14.2) when simple rectangular geometries are considered.

The paper is organised as follows. In §14.2 we employ the collocation technique to obtain a set of equations that can be solved to approximate the NFM in Equation (14.2). Then in §14.3, we consider the effect of mesh regularity on the accuracy of our solutions, and perform a comparative analysis against more standard techniques, deploying either trapezoidal rule or Fourier based techniques to compute the convolution integral in (14.2), in the case of a regular grid. We finish in §14.4 by giving an overview of the work as well as explaining its possible implications, before outlining a number of possibilities for future work.

14.2   The collocation method

Collocation is an example of a projection method that approximates an infinite dimensional problem, such as (14.2), by a finite dimensional one via a suitably defined projection operator $\mathcal{P}_n$. In what follows we provide brief details of the method as applied to Equation (14.2) (further details can be found in [7]).
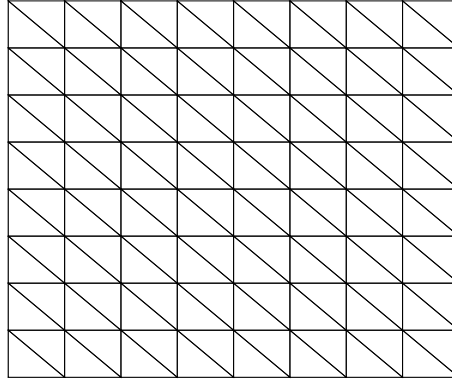
Figure 14.1: Illustration of a domain that uses Cartesian grid points as triangle vertices.

Consider the following triangulation $\mathcal{T}_n = \{\triangle_1, ..., \triangle_n\}$ of the square $[-L, L]^2$ and suppose that on each triangle $\triangle_k$ we employ a piecewise polynomial approximation of the unknown functions $u(x, y, t)$ and $a(x, y, t)$. In this case the projection operator takes the form

$$
\begin{aligned}
\mathcal{P}_n u(x, y, t) &= u_n(x, y, t) \\
&= \sum_{j=1}^{d} u(v_{k,j}, t) l_j(x, y), \quad \text{for } (x, y) \in \Delta_k, \ k = 1, 2, ..., n.
\end{aligned}
$$

Here, $v_{k,j}$ denotes the (x, y) coordinates of the jth interpolation point of the kth triangle, the l_j are the corresponding Lagrange basis functions, and d denotes the number of interpolation nodes. In this study we take $d = 3$ or 6 depending upon whether linear or quadratic interpolation is applied, respectively.

The above allows us to formulate the following approximation to (14.2):

$$
\begin{aligned}
\frac{\partial u_n(x, y, t)}{\partial t} &= A \mathcal{P}_n \left\{ \int_{-L}^{L} \int_{-L}^{L} w(x - x', y - y') S(u - h) \mathrm{d}x' \mathrm{d}y' \right\} \\
&\quad - u_n(x, y, t) - a_n(x, y, t), \\
\tau \frac{\partial a_n(x, y, t)}{\partial t} &= B u_n(x, y, t) - a_n(x, y, t).
\end{aligned}
\tag{14.3}
$$

Assuming this expression holds exactly at the node values $v_1, v_2, ..., v_{n_v}$, where n_v refers to the total number of globally indexed node points $v_{k,j}$, we obtain a collocation scheme for (14.2).

To make the above collocation scheme more tractable we perform the integration in (14.3) by applying a quadrature rule over each triangle and summing the result. More specifically, we employ the transformation $T_k : \sigma \to \triangle_k$, given by

$$
(x, y) = T_k(r, s) = (1 - r - s) v_{k,1} + s v_{k,2} + r v_{k,3},
\tag{14.4}
$$

which maps the unit simplex σ on to each triangle $\triangle_k$. This enables us to integrate an arbitrary function, g say, over the triangle $\triangle_k$ as follows

$$
\int_{\triangle_k} g(x, y) \mathrm{d}x \mathrm{d}y = 2 \text{Area}(\triangle_k) \int_{\sigma} g(T_k(r, s)) \mathrm{d}r \mathrm{d}s.
$$

Substituting this expression into (14.3) gives

$$
\begin{aligned}
\frac{\mathrm{d}u_n(v_i)}{\mathrm{d}t} &= 2A\sum_{k=1}^{n_t}\mathrm{Area}(\triangle_k)\int_\sigma w(v_i - T_k(r,s))S\left(\sum_{j=1}^d u(v_{k,j})l_j(r,s) - h\right)\mathrm{d}r\mathrm{d}s \\
&\quad - u_n(v_i) - a_n(v_i), \\
\tau\frac{\mathrm{d}a_n(v_i)}{\mathrm{d}t} &= Bu_n(v_i) - a_n(v_i),
\end{aligned}
\tag{14.5}
$$

for $i = 1, ..., n_v$ which is a system of $2n_v$ ordinary differential equations that can be solved to determine approximate solutions to (14.2).

14.3   Error analysis

When considering the numerical solution of Equation (14.2) the main source of error is the convolution integral and so we shall focus our analysis on the accurate representation of the integral

$$
I = \int_{-L}^{L}\int_{-L}^{L} w(x - x', y - y')S(u(x', y') - h)dx'dy',
\tag{14.6}
$$

in the remainder of the paper.

We compare the accuracy of both linear and quadratic collocation against fast Fourier transform (FFT) techniques together with the convolution theorem, and the trapezoidal method, both of which require a regular spatial discretisation such as the one displayed in Figure 14.1. To probe grid convergence, we consider a sequence of refinements of an initial, regular grid consisting of $N_0 = 81$ nodes, such that at the mth stage of refinement, the number of nodes is given by $N_m = (2^m \cdot 8 + 1)^2$ for $m = 1, 2, \ldots, 7$. If we then denote by I_m the numerical approximation of (14.6) on the grid of size N_m, we can approximate the order of convergence of the respective discretisation schemes by considering a log-log plot of the absolute error between consecutive grids $|I_m - I_{m+1}|$ versus grid size N_{m+1}. Here we consider point-wise convergence and so all results shown are for a representative grid point. Note that we have repeated the analysis for other grid points and observed almost identical behaviour (experiments not shown).

Our results are displayed in figures 14.2 and 14.3. In particular, from Figure 14.2 we see that both trapezoidal rule and FFTs display geometric convergence, as expected (see [8] for a discussion of the convergence properties of the trapezoidal rule on a periodic domain); however, we find, perhaps somewhat surprisingly, that linear collocation also exhibits geometric convergence. This is in contrast to quadratic collocation, which converges quadratically. To understand the above result, we consider the collocation technique as applied to (14.6) in more detail below.

Firstly, note that employing linear collocation alongside the three point quadrature rule

$$
\int_\sigma G(r,s)\mathrm{d}r\mathrm{d}s = \frac{1}{6}[G(0,0) + G(0,1) + G(1,0)],
$$

with $G(r,s) = g(T_k(r,s))$, as defined in §14.2, enables us to construct the following approxima-
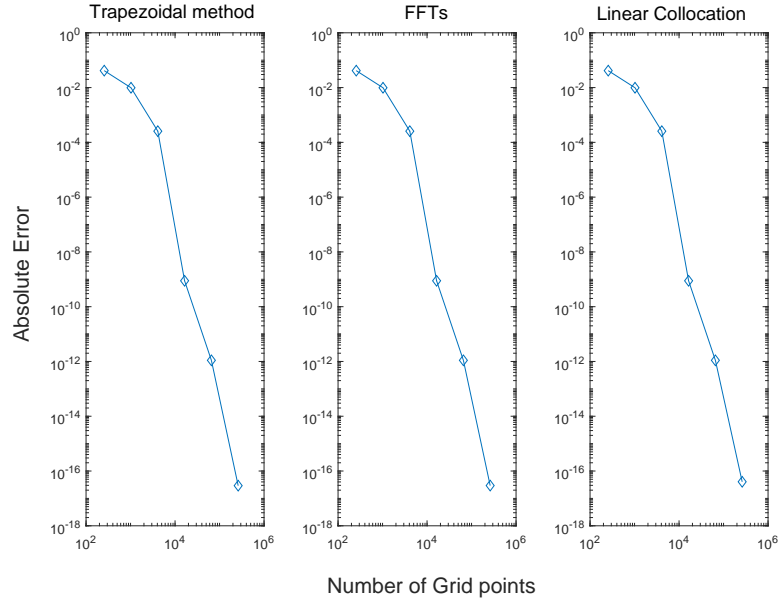
Figure 14.2: The error $|I_m - I_{m+1}|$ plotted against grid size N_{m+1} reveals geometric convergence rates for trapezoidal rule, FFTs and linear collocation when computing the integral in (14.6).

tion to (14.6):

$$I \approx \frac{1}{3} \sum_{k=1}^{n} \text{Area}\,(\Delta_k) \left[w(v - T_k(0,0))S \left(\sum_{j=1}^{3} u(v_{k,j})l_j(0,0) - h \right) + \right.$$

$$w(v - T_k(0,1))S \left(\sum_{j=1}^{3} u(v_{k,j})l_j(0,1) - h \right) + \qquad (14.7)$$

$$\left. w(v - T_k(1,0))S \left(\sum_{j=1}^{3} u(v_{k,j})l_j(1,0) - h \right) \right].$$

We can further simplify the above by noting that since we are solving on a uniform Cartesian domain, $\text{Area}\,(\Delta_k) = \Delta x^2/2$ for all triangles, where here, $\Delta x\,(= \Delta y)$ is the local mesh spacing. Substituting this into (14.7) and evaluating the Lagrange basis functions at the node points gives

$$\frac{\Delta x^2}{6} \sum_{k=1}^{n} \left[w(v - T_k(0,0))S(u(v_{k,1}) - h) + w(v - T_k(0,1))S(u(v_{k,2}) - h) \right.$$

$$\left. + w(v - T_k(1,0))S(u(v_{k,3}) - h) \right].$$

Recalling that $T_k(0,0)$ denotes the coordinates of the first vertex in Δ_k, $T_k(0,1)$ the second and
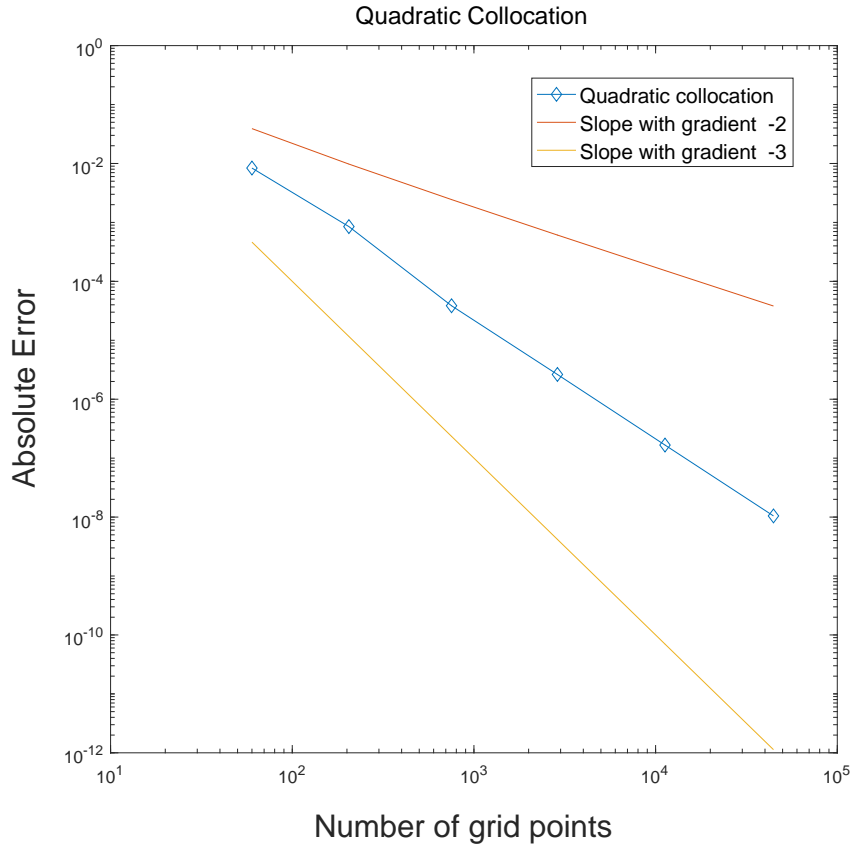
Figure 14.3: Convergence of quadratic collocation when computing the integral in (14.6) with the error $|I_m - I_{m+1}|$ plotted against grid size N_{m+1}.

$T_k(1,0)$ the third, we can rewrite the above as

$$
\frac{\Delta x^2}{6} \sum_{k=1}^{n} \Bigg[w(v - v_{k,1})S(u(v_{k,1}) - h) + w(v - v_{k,2})S(u(v_{k,2}) - h) \\
+ w(v - v_{k,3})S(u(v_{k,3}) - h) \Bigg]. \tag{14.8}
$$

However, for a regular grid the triangle vertices are simply the Cartesian mesh points and so Equation (14.8) is nothing other than the trapezoidal rule for solving (14.6) on a periodic two-dimensional domain. The factor of 1/6 occurs due to the fact that each node appears six times in the sum in (14.8). Thus, we have shown that for a regular grid with periodic boundary conditions solving Equation (14.6) using linear collocation and a quadrature rule based only on the triangle vertices is equivalent to using the trapezoidal rule. This explains the spectral convergence observed in Figure 14.2.

Next we consider the effects of mesh regularity on solutions of Equation (14.6). To do this we deployed the DistMesh Matlab package [9] to generate a general mesh, that is, one in which the triangle vertices do not lie on a Cartesian grid, as in our previous investigations. As before, numerical errors were approximated by comparing the numerical solution of (14.6) at the same grid point across a range of increasingly fine meshes. A refined triangulation was created by subdividing each triangle into four similar triangles, as shown in Figure 14.4. Results for linear and quadratic collocation are displayed in Figure 14.3. Note that in contrast to earlier results,
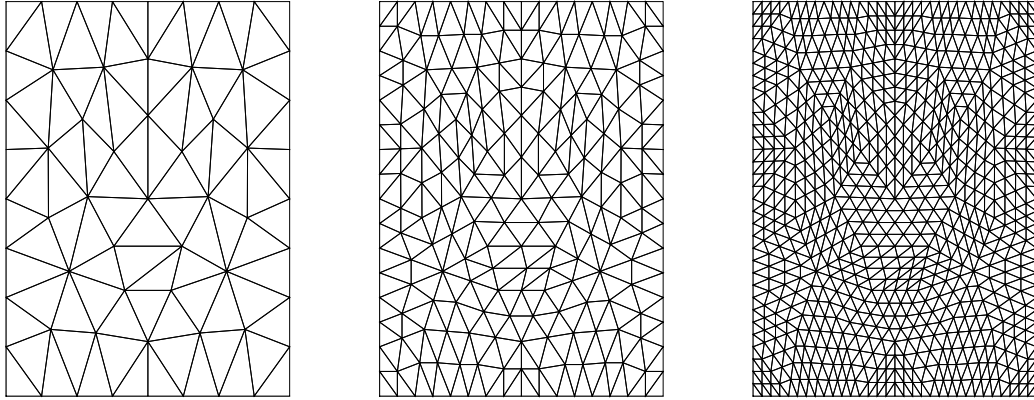
Figure 14.4: An illustration of the refinement procedure for a general triangulated domain. Meshes are generated using the DistMesh Matlab package [9].
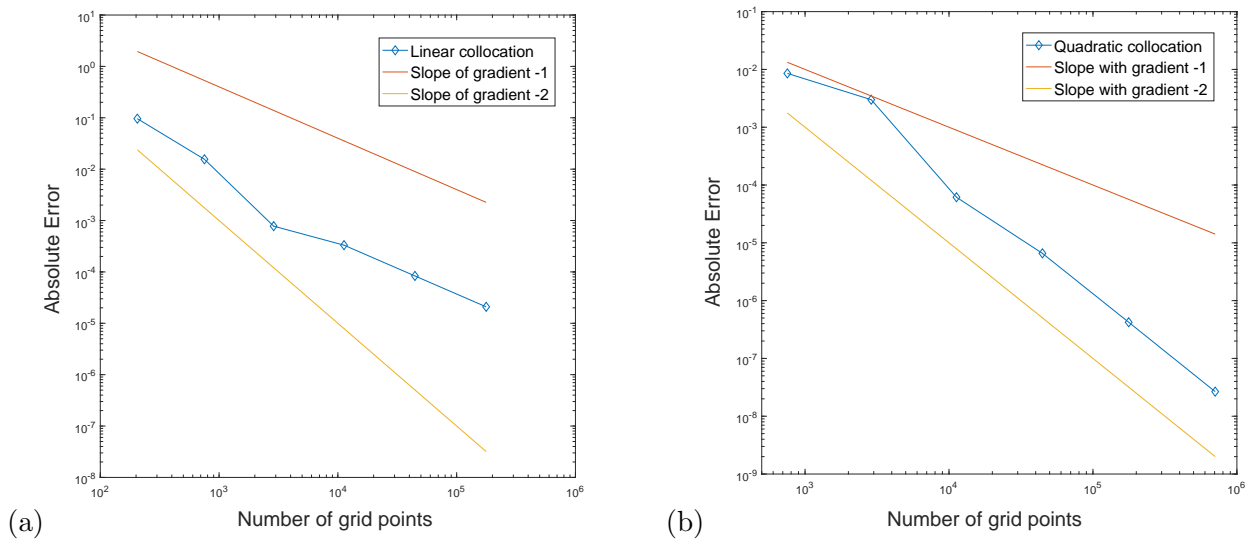

(a)   (b)

Figure 14.5: Convergence of (a) linear and (b) quadratic collocation when computing the integral in (14.6) using a general triangulation (see Figure 14.1).

superior convergence is now observed for quadratic collocation: linear and quadratic convergence is attained for linear and quadratic collocation, respectively. Thus, the geometric convergence displayed previously breaks down for more general triangulations, as expected.

14.4 Conclusions

In this work, we have employed collocation techniques to solve a two-dimensional NFM on a periodic, square domain $\Omega = [-L, L]^2$. Importantly, we found that these techniques were capable of reproducing solutions found by standard methods, which compute the convolution integral in the NFM using either Fourier based methods or the trapezoidal rule. Moreover, we found that when employing a regular triangulation based upon a Cartesian grid then, perhaps surprisingly, linear collocation out performed quadratic collocation. In fact, the linear collocation scheme was found to exhibit spectral convergence, similar to the Fourier based and trapezoidal methods. This result can be explained by noting that for a regular mesh with periodic boundary conditions, linear collocation can be shown to be equivalent to the trapezoidal rule for the particular quadrature methods employed here. For more general meshes the behaviour of lin-

ear and quadratic collocation was as expected, that is convergence was linear and quadratic, respectively. Future work shall deploy the methods discussed here, in conjunction with efficient numerical schemes for computing geodesic distances, to solve NFMs on two-dimensional curved geometries such as a sphere or torus. The overarching aim will be to extend these methods to more physiologically realistic cortical domains [10, 11, 12].

Acknowledgement

References

[1] P. C. BRESSLOFF, *Spatiotemporal dynamics of continuum neural fields*, Journal of Physics A: Mathematical and Theoretical, 45(3) (2011), 033001.

[2] S. COOMBES, *Large-scale neural dynamics: simple and complex*, Neuroimage, 52(3) (2010), 731–739.

[3] I. BOJAK, *et al.*, *Towards a model-based integration of coregistered electroencephalography/functional magnetic resonance imaging data with realistic neural population meshes*, Phil. Trans. R. Soc. A, 369, (2011), 3785-3801.

[4] P. SANZ-LEON, *et al.*, *Mathematical framework for large-scale brain network modelling in the virtual brain*, Neuroimage, 111 (2015), 385–430.

[5] C. R. LAING, *Neural Field Theory*, Springer, Berlin, 2013.

[6] C. R. LAING, *Numerical bifurcation theory for high-dimensional neural models*, Journal of Mathematical Neuroscience, 4 (2014), 13.

[7] K. E. ATKINSON, *The Numerical Solution of Integral Equations of the Second Kind*, Cambridge University Press, Cambridge, UK, 1997.

[8] L. N. TREFETHEN AND J. A. C. WEIDEMAN, *The exponentially convergent trapezoidal rule*, SIAM Review, 56(3) (2014), 385–458.

[9] P. O. PERSSON AND G. STRANG, *A simple mesh generator in MATLAB*, SIAM Review, 46(2) (2004), 329–345.

[10] R. O'DEA, *et al.*, *Spreading dynamics on spatially constrained complex brain networks*, Journal of the Royal Society Interface, 10 (2013), 20130016.

[11] J. A. HENDERSON AND P. A. ROBINSON, *Relations between geometry of cortical gyrification and white matter network architecture*, Brain Connectivity, 4 (2014), 112–130.

[12] Y-P. LO, *et al.*, *A geometric network model of intrinsic grey-matter connectivity of the human brain*, Scientific reports, 5 (2015), 15397.